# A Joint Modulation-Coding Scheme and Resource Allocation in LTE Uplink

Amado Gutierrez[1, *], Victor Rangel[1], Javier Gomez[1], Robert M. Edwards[2], David H. Covarrubias[3]
[1]*Engineering Faculty, National Autonomous University of Mexico,*
*Building Q-Valdés Vallejo, CP. 04510, CDMX Mexico*
[2]*5G Research Centre, Loughborough University,*
*LE11 3TU, UK*
[3]*Electronics and Telecommunications Department, CICESE Research Centre,*
*Ensenada-Tijuana Highway No. 3918, CP. 22860, Ensenada, B. C. Mexico*
*agg_telecom@comunidad.unam.mx*

***Abstract*—In Long Term Evolution (LTE) Resource Allocation Algorithms (RAAs) are an area of work where researchers are seeking to optimize the efficient use of scarce radio resources. The selection of an optimal Modulation and Coding Scheme (MCS) that allows LTE to adapt to channel conditions is a second area of ongoing work. In the wireless part of LTE, these two factors, RAA and MCS selection, are the most critical in optimization. In this paper, the performance of three resource allocation schemes is compared, and a new allocation scheme, Average MCS (AMCS) allocation, is proposed. AMCS is seen to outperform both "Minimum MCS (MMCS)" and "Average Signal to Interference and Noise Ratio MCS (SINR AMCS)" in terms of improvements to LTE Uplink (UL) performance. The three algorithms were implemented in the Vienna LTE-A Uplink Simulator v1.5.**

***Index Terms*—Resource allocation; Scheduling algorithms; Modulation coding; LTE-A; SC-FDMA; 3GPP.**

## I. INTRODUCTION

Scheduling algorithms for long term evolution (LTE) were not specified in the 3GPP standard and are, therefore, a matter for the suppliers. Rather than the Hybrid Frequency Division Multiple Access (FDMA)-Time Division Multiple Access (TDMA) used in 2G and the spreading codes and pseudo-random noise used in 3G, 4G LTE, LTE-A, and 5G New Radio (NR) [1], Orthogonal Frequency Division Multiplexing (OFDM) as their downlink modulation technology is used in [2]. However, since OFDM has a high peak to average power ratio (PAPR), it is considered unsuitable for the uplink in LTE, and therefore single carrier-frequency division multiple access (SC-FDMA) [3] that has lower PAPR was used. Both OFDM and SC-FDMA allocate resources to users with blocks of frequency and time called "physical resource blocks" (PRBs) [4] by the packet scheduler (PS).

Manuscript received 19 December, 2019; accepted 12 August, 2020.

This work was supported by DGAPA, National Autonomous University of Mexico (UNAM) under grants No. PAPIIT IN 116316, IN 117017, Doctoral fellowship CONACYT Grant No. CVU 227350. In addition, this research was funded by the Engineering and Physical Sciences Research Council (EPSRC) under Grant No. EP/P029221/1 and the Project SECTEI-CDMX: SECTEI/200/2019.

The PS is a crucial factor that allows the maximization of the LTE system performance [5] through optimal resource allocation. Several studies have divided the PS into two steps [6], [7]: 1) a time-domain packet scheduler (TDPS) that selects a subset of active users based on their priority and service quality (QoS), 2) a frequency-domain packet scheduler (FDPS) that allocates physically PRBs to each user in each transmission time interval (TTI) with one-millisecond duration [8]. Also, modulation and coding scheme (MCS) is another crucial factor that determines the data rate and the number of bits that can be transported in a PRB.

The user equipment (UE) sends sounding reference signals (SRSs) to the enhanced node base (eNB) to estimate channel quality. Then, the eNB uses the channel estimation to compute signal to interference and noise ratio (SINR) of all subcarriers of each UE. Moreover, the eNB uses the SINR values to generate PRBs and the link adaptation (LA) corresponding to each UE. With all information processed by the eNB, the channel-dependent scheduler (CDS) allocates PRBs and an MCS to a UE based on the highest SINR values and the mapping of the SINR with the channel quality indicator (CQI), respectively.

Unlike OFDM, to reduce PAPR, SC-FDMA has two constraints: PRBs allocated to a single user must be adjacent to each other and adjacent PRBs already assigned to a user must use the same channel quality indicator (CQI) index provided by MCS.

There are few studies focused on the performance of joint MCS and PRBs assignment for the LTE UL. In [9], a downlink (DL) FDPS, together with the MCS assignment algorithm, provide system reliability by the allocation of a lower order MCS to users who have poor channel quality. Nevertheless, the DL FDPS does not comply with the contiguity constraint of a UL FDPS. In [10]–[12], resource allocation algorithms were implemented for LTE UL under the minimum MCS constraint. However, the MCS was only used to guarantee the data transmission. The study of several FDPSs was presented in [13]–[15] for LTE UL, and all studied algorithms comply with the adjacency constraint. The results have shown that the Recursive Maximum

Expansion (RME) algorithm with the proportional fair (PF) metric present an excellent performance under the channel-dependent resource allocation scheme. However, these studies do not address their analysis on the MCS allocation, and the CQI is based on a worse channel condition of all its allocated PRBs. This means that the MCS allocation does not reach a flexible distribution of data rate in the assigned adjacent PRBs to a user. Besides, the studies, as mentioned earlier, are based on system-level simulations. This type of simulations does not allow a survey at subcarrier level of the LA for LTE UL. On the other hand, there is no analysis of the LA under a scenario with fast fading. Table I shows a comparative analysis of the revised literature.

TABLE I. COMPARATIVE TABLE OF THE STATE-OF-THE-ART.

| Papers | MCS allocation | LA | Scenario with fast fading and mobility | Analysis at link level | Link |
|---|---|---|---|---|---|
| [9] | Minimum SINR | Yes | No | No | DL |
| [10] | Minimum SINR | Yes | No | No | UL |
| [11] | Minimum SINR | Yes | No | No | UL |
| [12] | Minimum SINR | Yes | No | No | UL |
| [13] | No allocation | No | No | No | UL |
| [14] | No allocation | No | No | No | UL |
| [15] | No allocation | No | No | No | UL |
| AMCS Proposed | Allocation based on all SINR values | Yes | Yes | Yes | UL |

Currently, 5G NR will provide support to high-speed vehicular networks (HSVN), smart grid (SG), wireless control (WG), and automation in industrial environments (AIE) [16]. In all these scenarios, the UL is used to send collision risk warnings, energy consumption reports, commands to control drones, information about remote surgical operations, and manufacturing equipment. These reports are critical for avoiding accidents in highways, billing, manufacturing production quickly and accurately, and surgeries to patients in other parts of the world. However, the information is transmitted over a wireless channel, where there are low levels of SINR due to noise, fast and slow fading [17], [18], and Doppler effects. Consequently, FDPS study on the UL is crucial since it assigns the data rate to the PRBs that are most likely to carry information from UE to the eNB. Resource allocation to PRBs with poor channel quality contributes to loss of critical information and system performance degradation. For this reason, the motivation for this research topic is to improve the block-error rate (BLER) performance of the users that have poor channel quality due to fast and slow fading.

This paper examines the LA, FDPS, and MCS allocation to improve the link level throughput and decrease resource waste in environments with low SNR and considerable mobility. The LA used in this work is based in [19] and implemented in the LTE-A Uplink Link Level Simulator [20] downloadable at [21]. This simulator was implemented by the Institute of Telecommunications TU Wien to facilitate reproducibility in wireless communications academic research [22]. Using this approach, there have been several research works [23]–[26] that obtained their results from the Vienna simulator. The simulator works at the link level, which allows programming the schedulers at the subcarrier level in addition to modeling the link adaptation for LTE. It also uses SC-FDMA at the LTE uplink direction throughout different types of channels according to the 3GPP standard. All these characteristics allow the study of performance metrics in detailed way at PRBs and subcarriers level, which satisfy the requirements of the LTE standard. The LA allows adjusting the user's transmission rate according to the channel quality through 15 different MCSs linked by the CQI. The RME FPDS [13]–[15] is implemented in this work. RME is a heuristic algorithm and dependent channel [6] that complies with the contiguity constraint for LTE UL. Regarding the MCS allocation, MMCS, SINR AMCS, and AMCS are developed and analyzed in this work. The MCS is an essential tool that decides the achievable data rate and the amount of data that can be transported in a PRB. Consequently, the wrong choice of MCS leads to a degradation of the system throughput and severe waste of radio resources. Specifically, in environments with low SNR levels.

The main contributions of this paper are the following:

1. An improved link adaptation (ILA) for LTE uplink is proposed;
2. The AMCS that improves the reliability of information transmission of users that have weak quality channel is proposed;
3. Conduct link level simulations for LTE uplink to verify and study the results through a scenario with a low SINR, at considerable speed.

The remainder of this paper is organized as follows. Section II describes the LTE Uplink. Section III describes how to obtain the channel state matrix, including PRBs information. Section IV explains the RME algorithm. Section V details the MCS allocation with its different approaches to improve system performance. Section VI describes the simulation environment and results from the analysis. Section VII describes the discussion of results. Section VIII concludes the paper.

## II. LTE UPLINK

The sounding reference signal (SRS) is transmitted from the user equipment (UE) to the enhanced node base (eNB) covering all or part of the bandwidth to estimate the user's channel quality. When the SRS arrives at the eNB, it goes through various signal processing modules: OFDM demodulation, channel estimation, post-demodulation channel, signal to noise and interference ratio (SINR) estimation and link adaptation [27]. The eNB, through all the SRS processing, extracts near-instantaneous frequency-selective channel state information (CSI). From this information, the eNB obtains the SINR of all subcarriers for each UE to generate the channel state matrix (CSM) and perform link adaptation. Consequently, the resource allocation algorithm in the frequency domain uses the CSM to allocate PRBs to each user.

In contrast, MCS uses link adaptation to allocate the CQI to the PRBs assigned to each user. Then, the UE sends a buffer status report (BSR) to the eNB through a physical uplink shared channel (PUSCH), containing information about the bit rate and priority that request the UE. With this information, the eNB calculates the PRBs number and bit rate through FDPS and LA, respectively. The eNB sends a report of the assigned bit rate to the UE using the physical downlink control channel (PDCCH). Finally, the UE transmits data traffic on the LTE UL by physical uplink shared channel (PUSCH).

The CQI value is set according to the channel conditions. This value contains two types of information: modulation order (QPSK, 16-QAM or 64-QAM) and the effective code rate (ECR) [28]. Therefore, the rate matching adjusts the scale of the resulting coded bits taking into consideration the PRB grid and modulation order allocated by the scheduler according to the following equation

$$e_r = \log_2(M)\times(N_{PRBs}\times N_{SC}\times S_{OFDM} - S_{SRS} - S_{DMRS}), \quad (1)$$

where $M$ is the number of bits corresponding to the allocated MCS, $N_{PRBs}$ is the number of PRBs assigned to the user, $N_{SC}$ is the subcarrier number in the PRB, $S_{OFDM}$ is the OFDM symbol number, $S_{SRS}$ is the SRS symbol number, and $S_{DMRS}$ is the demodulation reference signal (DMRS). Furthermore, the rate matching adjusts the bit rate by the $ECR$ according to

$$\mathrm{ECR} = \frac{c_r}{e_r}, \quad (2)$$

where $c_r$ is the number of useful data $(N_{TB})$ plus 24-bits CRC [29], and $e_r$ is the number of output coded bits. Therefore, the $(N_{TB})$ is given as

$$N_{TB} = (\mathrm{ECR}\times e_r) - 24. \quad (3)$$

## III. PRBS GENERATION DESCRIPTION

The PRB generation process of a UE is shown in Fig. 1. The first step is to compute the mean value of each row (R) of the CSM.

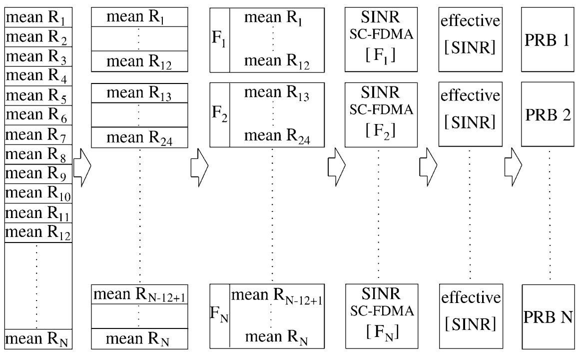


Fig. 1. PRBs generation of a UE.

The matrix contains the channel frequency response of all subcarriers of a UE with N subcarriers and 14 OFDM symbols. The second step groups the mean values in sets of 12 subcarriers [30]. The third step considers the equalization (F) proposed in [19] in the frequency domain for each set given as

$$\mathbf{F} = d\mathrm{diag}\left(\frac{\mathbf{H}_k^*}{|\mathbf{H}_k|^2 + \frac{\sigma_n^2}{\sigma_x^2}}\right), \quad (4)$$

where $\mathbf{H}$ is the channel frequency response, $k$ is the subcarrier index, $\sigma_n^2$ is the subcarriers noise power, and $\sigma_x^2$ is the subcarriers signal power.

The fourth step spreads the SINR to each set already equalized, which can be described as [19]

$$\mathrm{SINR}^{\text{SC-FDMA}} = \\ = \frac{\frac{\sigma_x^2}{12}|\mathrm{diag}(\mathbf{FH})|^2}{\sigma_x^2\|\mathbf{FH}\|^2 - \frac{\sigma_x^2}{12}|\mathrm{diag}(\mathbf{FH})|^2 + \mathbf{F}^T\mathbf{F} + (\sigma_n^2)\times\|\mathrm{diag}(\mathbf{F})\|^2}. \quad (5)$$

To obtain the LA, the fifth step gets the effective SINR by Exponential Effective SINR Mapping (EESM) [31] to compress the $SINRs^{SC\text{-}FDMA}$ into a single value equivalent to a SINR value of an Additive White Gaussian Noise (AWGN) channel. It is defined as

$$\mathrm{SINR}_{\mathrm{eff}} = \mathrm{EESM}(\mathrm{SINR},\beta) = -\beta l\ln\left(\frac{1}{N}\sum_{i=1}^{N} e^{-\frac{\mathrm{SINR}_i^{\text{SC-FDMA}}}{\beta}}\right), \quad (6)$$

where $N$ is the subcarrier number (i.e., resource element number) and $\beta$ is an empirical parameter used as a calibration factor, which is MCS dependent. The effective SINR gives rise to a PRB. Intending to form PRBs in a multiuser environment, the eNB server creates n-CSM when there are n-UEs in the cell. Also, the eNB must follow the procedure described in Fig. 1. The obtained PRBs are stored in a metrics matrix as illustrated in Fig. 2.

## IV. RESOURCES ALLOCATION ALGORITHM

The CDS allocates resources to UEs experiencing the best channel quality. This means that the scheduler will allocate a PRB to the UE with a higher $\mathrm{SINR}_{\mathrm{eff}}$ value.

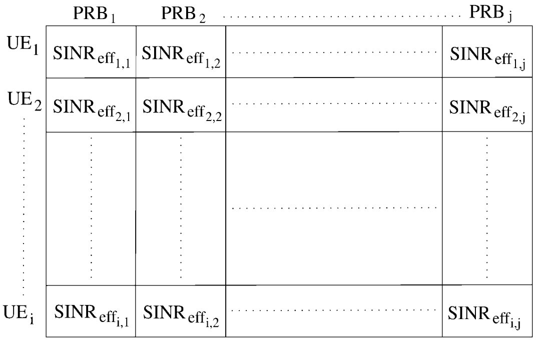


Fig. 2. Metrics matrix of UEs with its corresponding PRBs.

Also, the scheduler must consider the adjacency constraint. Consequently, the RME algorithm searches for the best UE-PRB pair with higher SINR value on the metrics matrix, and so it makes the first allocation $UE_0$-$RB_0$. Next, the $UE_0$ allocation expands up and down until it finds other $UE_i$ with a higher value. Right after this, $UE_0$ is set to idle mode. The algorithm repeats the previous process until all UEs are in idle mode or all PRBs have been assigned. When unassigned PRBs remain, the algorithm looks for the best $UE_i$-$PRB_j$ pair among all remaining PRBs. The $PRB_j$ allocation occurs when: a) the $PRB_j$ is adjacent to the already allocated PRBs to the $UE_i$ that is in idle mode, b) the next closest $PRB_j$ is far away from the previously allocated PRBs to the $UE_i$. The allocation expands until it reaches the contiguity, and on the opposite side until it finds other UE (idle) with higher metric value. An example of how the RME algorithm allocated PRBs to the users using this procedure is shown in Table II.

TABLE II. ASSIGNED PRBS.

| PRB | Subcarriers | UE1 SINR | UE2 SINR | UE3 SINR | Allocation |
|---|---|---|---|---|---|
| PRB1 | 1, …, 12 | 7.03 | 3.53 | 1.44 | UE3 |
| PRB2 | 13, ..., 24 | 11.76 | 3.51 | 3.19 | UE3 |
| PRB3 | 25, …, 36 | 7.89 | 2.91 | 4.37 | UE3 |
| PRB4 | 37,…,48 | 4.41 | 4.89 | 6.83 | UE3 |
| PRB5 | 49, …, 60 | 10.77 | 7.46 | 4.14 | UE3 |
| PRB6 | 61, …, 72 | 10.43 | 6.63 | 7.30 | UE3 |
| PRB7 | 73, …, 84 | 3.37 | 9.63 | 11.02 | UE3 |
| PRB8 | 85, …, 96 | 10.47 | 8.93 | 12.59 | UE3 |
| PRB9 | 97, …, 108 | 14.58 | 6.43 | 13.15 | UE1 |
| PRB10 | 109, …, 120 | 9.52 | 19.81 | 11.53 | UE2 |
| PRB11 | 121,…,132 | 7.28 | 40.36 | 9.16 | UE2 |
| PRB12 | 133, …, 144 | 13.35 | 38.53 | 4.86 | UE2 |
| PRB13 | 145, …, 156 | 9.24 | 37.93 | 8.45 | UE2 |
| PRB14 | 157, …, 168 | 0.97 | 39.74 | 7.47 | UE2 |
| PRB15 | 169, …, 180 | 2.72 | 25.03 | 6.52 | UE2 |

## V. MCS ALLOCATION

### A. Vienna MCS and LA Allocation Description

Vienna MCS allocation [19] is based in (7) and (8). For instance, $UE_3$, $UE_1$, and $UE_2$ have received eight, one, and six PRBs, respectively. The position of these are $PRB_1$–$PRB_8$, $PRB_9$, and $PRB_{10}$–$PRB_{15}$, respectively, and the subcarriers are $\overline{R}_1-\overline{R}_{96}$, $\overline{R}_{97}-\overline{R}_{108}$, and $\overline{R}_{109}-\overline{R}_{180}$ as shown in Table II. These subcarriers are taken from CSM of each UE; it can be represented as:

$$\left\{ \mathbf{CSM}_3=\begin{bmatrix}\overline{R}_1\\ \vdots\\ \overline{R}_{96}\\ \overline{R}_{97}\\ \vdots\\ \overline{R}_{108}\\ \overline{R}_{109}\\ \vdots\\ \overline{R}_{180}\end{bmatrix}, \mathbf{CSM}_1=\begin{bmatrix}\overline{R}_1\\ \vdots\\ \overline{R}_{96}\\ \overline{R}_{97}\\ \vdots\\ \overline{R}_{108}\\ \overline{R}_{109}\\ \vdots\\ \overline{R}_{180}\end{bmatrix}, \mathbf{CSM}_2=\begin{bmatrix}\overline{R}_1\\ \vdots\\ \overline{R}_{96}\\ \overline{R}_{97}\\ \vdots\\ \overline{R}_{108}\\ \overline{R}_{109}\\ \vdots\\ \overline{R}_{180}\end{bmatrix}\right\}. \quad (7)$$

where $\overline{R}$ is a subcarrier based on the mean value of each row of the corresponding UE CSM. To obtain the CQI value and, consequently, the MCS scheme, the LA is based on (4), (5), and (6). For instance, for $UE_3$, it can be represented as:

$$\begin{cases} \mathbf{F}\begin{bmatrix}\overline{R}_1\\ \vdots\\ \overline{R}_{96}\end{bmatrix},\\ \mathbf{SINR}^{\mathbf{SC-FDMA}}\begin{bmatrix}F_1\\ \vdots\\ F_{96}\end{bmatrix},\\ \mathbf{Effec\_SINR}\begin{bmatrix}S\,\mathrm{SINR}_1^{\text{SC-FDMA}}\\ \vdots\\ \mathrm{SINR}_{96}^{\text{SC-FDMA}}\end{bmatrix},\\ \mathbf{value\_CQI}=[\text{Effect\_SINR}]. \end{cases} \quad (8)$$

The CQI value is obtained through an allocation process by using (8). In case there are n-UEs, the process would be repeated n-times. In (8), the equalization is applied to all subcarriers of the $UE_3$. Consequently, the subcarriers with the highest SINR value have greater weight than the subcarriers with a lower SINR value. Due to this, the CQI assignment is focused on the weight of the highest effective SINR values. Therefore, subcarriers with poor channel quality get a more significant number of bits that cannot support. Due to the constraint of LTE uplink, this behavior leads to a degradation of throughput and a waste of resources in an environment where the SINR values are critical.

### B. MMCS and SINR AMCS Allocation Description and Improved LA

To implement the MMCS, SINR AMCS, and AMCS, the following link adaptation process is developed:

$$\begin{cases} \mathbf{CSM}_3=\begin{bmatrix}\overline{R}_1,\cdots,\overline{R}_{12}\\ \overline{R}_{13},\cdots,\overline{R}_{24}\\ \vdots\\ \overline{R}_{85},\cdots,\overline{R}_{96}\end{bmatrix},\\ \mathbf{CSM}_1=\left[\overline{R}_{97},\cdots,\overline{R}_{108}\right],\\ \mathbf{CSM}_2=\begin{bmatrix}\overline{R}_{109},\cdots,\overline{R}_{120}\\ \overline{R}_{121},\cdots,\overline{R}_{132}\\ \vdots\\ \overline{R}_{169},\cdots,\overline{R}_{180}\end{bmatrix}. \end{cases} \quad (9)$$

For instance, for $UE_3$ of $CSM_3$ from (9) it can be represented as:

$$\begin{cases} \mathbf{F}\begin{bmatrix}\overline{R}_1,\dots,\overline{R}_{12}\\ \overline{R}_{13},\dots,\overline{R}_{24}\\ \vdots \\ \overline{R}_{85},\dots,\overline{R}_{96}\end{bmatrix}, \\ \mathbf{SINR}^{SC-FDMA}\begin{bmatrix}F_1(1),\dots,F_1(12)\\ F_2(1),\dots,F_2(12)\\ \vdots \\ F_8(1),\dots,F_8(12)\end{bmatrix}, \\ \mathbf{Effec\_SINR}\begin{bmatrix}SINR_1^{SC-FDMA}(1),\dots,SINR_1^{SC-FDMA}(12)\\ SINR_2^{SC-FDMA}(1),\dots,SINR_2^{SC-FDMA}(12)\\ \vdots \\ SINR_8^{SC-FDMA}(1),\dots,SINR_8^{SC-FDMA}(12)\end{bmatrix}, \\ \mathbf{value\_CQI} = \left[Effec\_SINR_1,\dots,Effec\_SINR_8\right]. \end{cases} \quad (10)$$

In (10), the equalization is applied in groups of 12 subcarriers. Consequently, the weight of the subcarriers with a low SINR value is spread in each group. This means that the subcarriers with the highest SINR value have affected a small group of subcarriers with the lowest SINR value. Otherwise, if a group has more subcarriers with poor channel quality, it will have a low effective SINR value. Therefore, the procedure presented in (10) has better diversity than in (8) due to the fact that subcarriers with a poor channel quality affect only on a group of 12 subcarriers. Besides, this approach allows a better allocation of CQI to improve the system throughput and waste of resources.

From (5) and (6), under environments with low SINR, the $SINR^{SC\text{-}FDMA}$ obtains positive values of SINR, while the effective SINR leads to positive and negative values of SINR. The MMCS allocates the CQI value to a UE based on its PRB with lowest effective SINR; it can be represented as

$$\mathbf{value\_CQI} = \mathbf{Min}\left[Effec\_SINR_1,\dots,Effec\_SINR_8\right]. \quad (11)$$

To study the behavior of the CQI allocation under the $SINR^{SC\text{-}FDMA}$, the SINR AMCS is proposed in (12). This scheme allocates the CQI value to a UE with an average cost; it can be represented as

$$\mathbf{value\_CQI} = \mathbf{Mean}\left[SINR_1^{SC\text{-}FDMA},\dots,SINR_8^{SC\text{-}FDMA}\right]. \quad (12)$$

Both MMCS and SINR AMCS compute the MCS by the SINR-CQI mapping shown in Table III.

TABLE III. SUPPORTED MCS INDEX AND ASSOCIATED SINR-CQI.

| MCS | CQI | SINR [dB] | Modulation | Code Rate x 1024 | Efficiency |
|---|---|---|---|---|---|
| [4], [32] | [32] | [12], [33] | [32] | [32], [34] | [32], [34] |
| - | 0 | Out Range | | | |
| - | 1 | -7.0 → -5.0 | QPSK | 78 | 0.1523 |
| 0 | 2 | -5.0 → -3.0 | QPSK | 120 | 0.2344 |
| 1 | | | QPSK | | |
| | | | | | |
| 2 | 3 | -3.0 → -1.0 | QPSK | 193 | 0.3770 |
| 3 | | | QPSK | | |
| 4 | 4 | -1.0 → +1.0 | QPSK | 308 | 0.6016 |
| 5 | | | QPSK | | |
| 6 | 5 | +1.0 → +3.0 | QPSK | 449 | 0.8770 |
| 7 | | | QPSK | | |
| 8 | 6 | +3.0 → +5.0 | QPSK | 602 | 1.1758 |
| 9 | | | QPSK | | |
| 10 | | | 16 QAM | | |
| 11 | 7 | +5.0 → +7.0 | 16 QAM | 378 | 1.4766 |
| 12 | | | 16 QAM | | |
| 13 | 8 | +7.0 → +8.5 | 16 QAM | 490 | 1.9141 |
| 14 | | | 16 QAM | | |
| 15 | 9 | +8.5 → +10.0 | 16 QAM | 616 | 2.4063 |
| 16 | | | 16 QAM | | |
| 17 | | | 64 QAM | | |
| 18 | 10 | +10.0 → +11.5 | 64 QAM | 466 | 2.7305 |
| 19 | | | 64 QAM | | |
| 20 | 11 | +11.5 → +13.5 | 64 QAM | 567 | 3.3223 |
| 21 | | | 64 QAM | | |
| 22 | 12 | +13.5 → +15.0 | 64 QAM | 666 | 3.9023 |
| 23 | | | 64 QAM | | |
| 24 | 13 | +15.0 → +17.0 | 64 QAM | 772 | 4.5234 |
| 25 | | | 64 QAM | | |
| 26 | 14 | +17.0→+19.5 | 64 QAM | 873 | 5.1152 |
| 27 | | | 64 QAM | | |
| 28 | 15 | +19.5 → ∞ | 64 QAM | 9480 | 5.5547 |
| 29 | | QPSK | | | |
| 30 | | 16 QAM | | Reserved | |
| 31 | | 64 QAM | | | |

## C. *AMCS Allocation Description*

In (11), the MMCS takes into account the minimum SINR value of all the assigned PRBs to the UE. However, MMCS does not consider other effective SINR values. Thus, there is a need for the scheduler to achieve a more rational and flexible distribution among effective SINR values. In (12), the proposed SINR AMCS computes the average of the values corresponding to each PRB. This scheme provides a high CQI due to the average of positive values, which means that a UE obtains a higher bit rate compared to MMCS and AMCS. However, in environments with fast fading, the PRBs with poor channel quality do not support high bit rate. Consequently, the transmission of critical information would be lost in addition to causing delays due to the retransmission of data.

Based on the analysis, as mentioned above, the AMCS allocation is proposed and adapted to improve the link level throughput and loss of radio resources. The AMCS considers the adjacency constraint and the LA presented in (10). Consequently, the contiguous PRBs allocation requires of a CQI value to obtain the data rate of a UE. Due to this, AMCS computes a fixed value of CQI for each contiguous

PRB by SINR-CQI mapping shown in Table III. Right after that, the average CQI values are calculated to obtain only a CQI value and allocates the corresponding MCS. For instance, for UE3, it can be represented as

$$\mathbf{UE}_3 = \begin{bmatrix} Effec\_SINR_1 \\ \vdots \\ Effec\_SINR_8 \end{bmatrix} = \begin{bmatrix} CQI_1 \\ \vdots \\ CQI_8 \end{bmatrix}. \quad (13)$$

To obtain the CQI value from (13), the average on the effective SINR of each PRB in (14) can be calculated

$$\mathbf{value\_CQI} = \mathbf{Mean}\left[\mathrm{CQI}_1, \ldots, \mathrm{CQI}_8\right]. \quad (14)$$

However, the proportion of the average of negative and positive values leads to low CQI.

The results of (8), (11), (12), and (14), together with RME algorithm, are illustrated in Fig. 3, which shows the assigned data rate by the scheduler where the SINR AMCS algorithm achieves a better data rate. However, SINR AMCS is not optimal in environments where the subcarriers have low SINR. But, this can be considered in scenarios with a good channel quality.

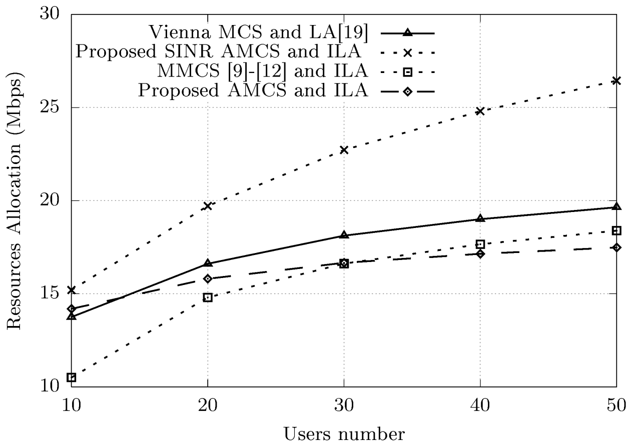


Fig. 3. Bit rate allocation to the users.

Figure 3 shows the resource allocation versus the number of users. When there are 50 users in the cell, the proposed SINR AMCS presents a considerable improvement compared with Vienna, MMCS, and proposed AMCS in 25 %, 30 %, and 33 %, respectively. The proposed SINR AMCS improved due to the average of the $SINR^{SC\text{-}FDMA}$ values from the LA. However, this does not mean an improvement in the system throughput at the link level. Specifically, in environments where there are a lot of abrupt changes due to a considerable speed and rapid fluctuations of the received signals in the time domain. All these characteristics give rise to a scenario with low SNR values and a high loss of radio resources.

Furthermore, when there are 50 users, the proposed AMCS presents less amount of resources allocation in 3.9 % compared with MMCS. The proposed AMCS showed the least amount of assigned resources due to the average applied to obtained CQI values of the SINR-CQI mapping. Hence, this work presents an analysis of system throughput, fairness, and BLER of the proposed algorithms in environments with low SNR, at considerable speed.

## VI. Simulations Results and Analysis

The proposed Vienna MCS, SINR AMCS, MMCS, and AMCS, together with the RME algorithm and link adaptation shown in (10), are implemented by the LTE Uplink Link Level Simulator v1.5. The wireless channel was modeled as an extended vehicular model A with nine paths [8]. Also, the FDD frame structure was used. All simulations ran with 1000 TTI, and the results were averaged out. Each user moves at a speed of 80 km/h with a channel bandwidth of 10 MHz. Channel estimation and filtering on the eNB were given by the minimum mean squared error (MMSE) and fast fading, respectively. The main simulation parameters are given in Table IV.

TABLE IV. PARAMETERS OF THE SIMULATION.

| Parameter | Value |
|---|---|
| Channel bandwidth | 10 MHz |
| Number of users | 10, 20, 30, 40, 50 |
| Minimum SNR value | 6 dB |
| Subframes (TTI) | 1000 |
| Channel model | EVehA of 9 Taps |
| Filtering | Fast Fading |
| Channel estimation | MMSE |
| Traffic | Full Buffer |
| Transmission frequency | 1700 MHz |
| User's speed | 80 km/h |

Based on the above simulation model, the performance of the proposed AMCS was compared to MMCS, proposed SINR AMCS, and Vienna MCS. All obtained results were evaluated under a scenario that suffers from low channel quality, at considerable speed. A wireless channel with an SNR of 6 dB provides a bad quality link in vehicle-to-infrastructure environments [35], [36]. For this reason, we have used an SNR of 6 dB in all simulations.

Figure 4 shows the link level throughput performance for all schemes versus the number of users.

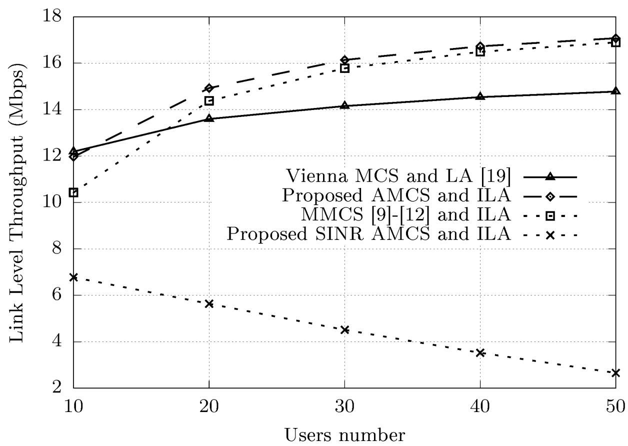


Fig. 4. Link level throughput with SNR = 6 dB.

A comparison of simulations results reveals that the performance of proposed AMCS and MMCS presents a 14 % and 11.4 % improvement compared to the Vienna MCS, respectively. A high loss of link level throughput for the proposed SINR AMCS can be observed for any number of users. This disparity is a consequence of the high number of assigned data bits to users in environments with adverse quality channel conditions.

Figure 5 shows fairness performance for all considered schemes. A maximum of 25 % and 16 % improvement can be observed for proposed AMCS and MMCS compared to Vienna MCS, respectively. The fairness analysis reveals that as the number of users increases, the proposed AMCS increases the fair value by up to 7 % compared to MMCS in a specific range. There is a fairness degradation for the proposed SINR AMCS due to considerable loss of data bits.

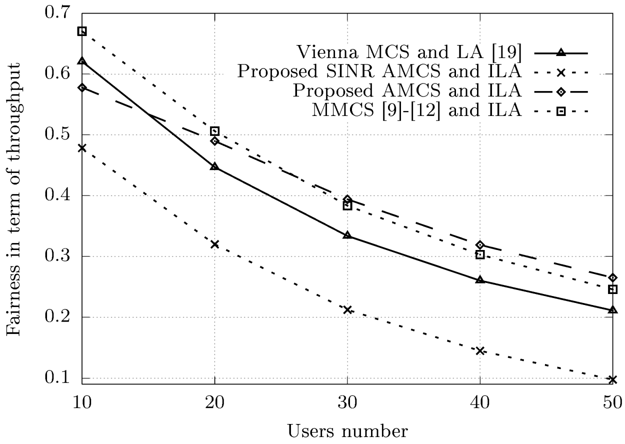


Fig. 5. Fairness in terms of throughput with SNR = 6 dB.

Figure 6 compares the block error rate versus the number of users in an environment with low SNR value at considerable mobility.

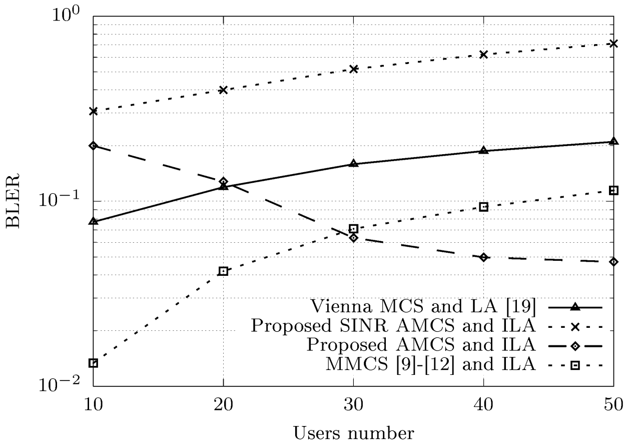


Fig. 6. Block error rate with SNR = 6 dB.

Based on the comparison of the obtained results, when the number of users increases above 30, the BLER of the proposed AMCS algorithm is better. It can thus be established that the proposed CQI allocation mechanism achieves a substantial improvement in terms of BLER, which can be up to 60 % for 50 users in the cell. The high bit rate loss in the results obtained for MMCS, Vienna MCS, and proposed SINR AMCS is the result of the inadequate allocation of the CQI value to the users in the cell. This is because, for scenarios with bad channel quality, the scheduler assigns more data bits throughout the average $SINR^{SC-FDMA}$ or minimum effective SINR. The proposed AMCS allocates CQI value to each effective SINR value. Then, calculates the average value of CQI to limit the bit allocation. Besides, using the link adaptation presented in (10) together with the RME algorithm improves the efficient use of resources.

Figure 7 shows the block error rate versus signal to noise ratio with 50 users in the cell. A considerably better BLER is achieved when the proposed AMCS is applied in environments with low SNR values and considerable speed. For a value of 10 % of the BLER, the proposed AMCS starts to decrease. Also, from SNR 4 dB to 10 dB, the proposed AMCS shows a better behavior compared to the other algorithms. It can be established that the proposed AMCS achieves a substantial improvement in terms of waste of radio resources. Consequently, the proposed CQI allocation mechanism in this work can be used in vehicular-to-infrastructure environments or scenarios that present a low SNR level. The set of measurement data is available in [37].

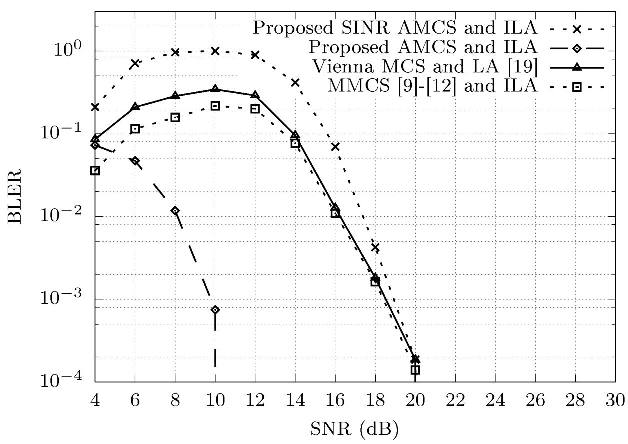


Fig. 7. Block error rate versus SNR for 50 users.

## VII. DISCUSSION

The selection of a link level simulator with an extended vehicular channel and the selected scenario allows for an exhaustive analysis of resources allocation and link adaptation at the subcarrier level. The results presented in this paper prove that the best performance is achieved with values of SNR from 4 dB to 10 dB. High waste of radio resources is more likely to occur in environments with poor channel quality, high speed, and low SNR values. This means that the proposed AMCS is useful when SNR values are low and the speed is high. Simulation results have also demonstrated that for a low SNR value of 6 dB, the link level throughput and fairness achieve better results, while the number of users is incremented. Moreover, with the new CQI allocation technique and the enhanced technique of link adaptation, the radio resource allocation in scenarios with poor channel quality and high speeds are ensured. Furthermore, the throughput improves by 3 % and fairness by 7 % due to the MCS allocation, which is based on the CQI average value of all subcarriers.

## VIII. CONCLUSIONS

In this paper, joint modulation-coding selection and radio resource allocation were considered for LTE uplink. The performance of three resource allocation schemes was compared, and a new allocation scheme, Average MCS (AMCS) allocation, was proposed, which, together with Recursive Maximum Expansion (RME) algorithm, have been implemented in an uplink link level simulator. The assignment of CQI values has been achieved to improve the efficiency of use of radio resources and maintain an excellent link level throughput considering constraints of uplink LTE. We have shown, through numerical simulation, that our proposed scheme technique improves the performance of users experiencing low SNR values, at considerable mobility, enhancing, besides network performance in terms of throughput, fairness, and BLER for a high number of users in a cell.

## CONFLICTS OF INTEREST

The authors declare that they have no conflicts of interest.

## REFERENCES


[1] A. A. Zaidi, R. Baldemair *et al.*, "OFDM numerology design for 5G new radio to support IoT, eMMB, and MBSFN", *IEEE Communications Standards Magazine*, vol. 2, no. 2, pp. 78–83, 2018. DOI: 10.1109/MCOMSTD.2018.1700021.

[2] Study on New Radio (NR) access technology, 3GPP TR38.912, v15.0.0, 2018.

[3] J. Ding, A. Roy, and N. Saxena, "Smart M2M uplink scheduling algorithm over LTE", *Elektronika ir Elektrotechnika*, vol. 19, no. 10, pp. 138–144, 2013. DOI: 10.5755/J01.EEE.19.10.5457.

[4] G. Ku and J. M. Walsh, "Resource allocation and link adaptation in LTE and LTE-A: A tutorial", *IEEE Communications Surveys & Tutorials*, vol. 17, no. 3, pp. 1605–1633, 2015. DOI: 10.1109/COMST.2014.2383691.

[5] M. Algharem, M. H. Omar, I. Aldmour, and R. Budiarto, "Multicast Resource Allocation with Opportunistic Scheduling in LTE Networks", *Elektronika ir Elektrotechnika*, vol. 24, no. 5, pp. 92–101, 2018. DOI: 10.5755/j01.eie.24.5.21850.

[6] H. Safa and K. Tohme, "LTE uplink scheduling algorithms: Performance and challenges", in *Proc. of IEEE 19th International Conference on Telecommunications (ICT 2012)*, 2012, pp. 1–6. DOI: 10.1109/ICTEL.2012.6221230.

[7] F. Capozzi, G. Piro, L. A. Grieco, G. Boggia, and P. Camarda, "Downlink packet scheduling in LTE cellular networks: Key design issues and a survey", *IEEE Communications Surveys & Tutorials*, vol. 15, no. 2, pp. 678–700, 2013. DOI: 10.1109/SURV.2012.060912.00100.

[8] User equipment (UE) radio transmission and reception for Evolved Universal Terrestrial Radio Access (E-UTRA), 3GPP TS 36.101, v10.4.0, 2011.

[9] D. Jianbo, Z. Liqiang, F. Jie, X. Jie, and W. Yong, "Enhanced PSO based energy-efficient resource allocation and CQI based MCS selection in LTE-A heterogeneous system", *IEEE China Communications*, vol. 13, no. 11, pp. 197–204, 2016. DOI: 10.1109/CC.2016.7781730.

[10] H. L. Chao, C. K. Chang, and C. L. Liu, "A novel channel-aware frequency-domain scheduling in LTE uplink", in *Proc. of IEEE Wireless Communications and Networking Conference*, 2013, pp. 917–922. DOI: 10.1109/WCNC.2013.6554686.

[11] L. H. Hsu and H. L. Chao, "On channel-aware frequency-domain scheduling with QoS support for uplink transmission in LTE systems", in *Proc. of IEEE Signal and Information Processing Association Annual Summit and Conference (APSIPA)*, 2013, pp. 1–6. DOI: 10.1109/APSIPA.2013.6694224.

[12] F. Z. Kaddour, E. Vivier, L. Mroueh, M. Pischella, and P. Martins, "Green opportunistic and efficient resource block allocation algorithm for LTE uplink networks", *IEEE Transactions on Vehicular Technology*, vol. 64, no. 10, pp. 4537–4550, 2015. DOI: 10.1109/tvt.2014.2365960.

[13] E. E. Tsiropoulou, A. Kapoukakis, and S. Papavassiliou, "Uplink resource allocation in SC-FDMA wireless networks: A survey and taxonomy", *ELSEVIER Computer Networks*, vol. 96, pp. 1–28, 2016. DOI: 10.1016/j.comnet.2015.12.006.

[14] N. Abu-Ali, A.-E. M. Taha, M. Salah, and H. Hassanein, "Uplink scheduling in LTE and LTE- Advanced: Tutorial, survey and evaluation framework", *IEEE Communications Surveys & Tutorials*, vol. 16, no. 3, pp. 1239–1265, 2014. DOI: 10.1109/surv.2013.1127.00161.

[15] L. A. M. Ruiz de Temiño, G. Berardinelli, S. Frattasi, and P. Mogensen, "Channel-aware scheduling algorithms for SC-FDMA in LTE uplink", in *Proc. of IEEE 19th International Symposium on Personal, Indoor, and Mobile Radio Communications (PIMRC 2008)*, 2008, pp. 1–6. DOI: 10.1109/pimrc.2008.4699645.

[16] G. Pocovi, K. I. Pedersen, and P. Mogensen, "Joint link adaptation and scheduling for 5G ultra-reliable low-latency communications", *IEEE Access*, vol. 6, pp. 28912–28922, 2018. DOI: 10.1109/access.2018.2838585.

[17] V. Markevicius, D. Navikas, D. Andriukaitis, M. Cepenas, A. Valinevicius, M. Zilys, R. Malekian, A. Janeliauskas, W. Walendziuk, A. Idzkowski, "Two thermocouples low power wireless sensors network", *AEU - International Journal of Electronics and Communications*, vol. 84, pp. 242–250, 2018. DOI: 10.1016/j.aeue.2017.11.032..

[18] L. T. T., Hoc, H.-S., Nguyen, Q.-P. Ma, V. V. Huynh, , *et al.*, "Outage and Bit Error Probability Analysis in Energy Harvesting Wireless Cooperative Networks", *Elektronika ir Elektrotechnika*, vol. 25, no. 5, pp. 69–74, 2019. DOI: 10.5755/j01.eie.25.5.24359.

[19] E. Zöchmann, S. Schwarz, S. Pratschner, L. Nagel, M. Lerch, and M. Rupp, "Exploring the physical layer frontiers of cellular uplink", *EURASIP Journal on Wireless Communications and Networking*, vol. 2016, no. 1, pp. 1–18, 2016. DOI: 10.1186/s13638-016-0609-1.

[20] M. Rupp, S. Schwarz, and M. Taranetz, *The Vienna LTE-Advanced Simulators: Up and Downlink, Link and System Level Simulation*, 1st ed. Singapore: Springer, 2016. DOI: 10.1007/978-981-10-0617-3.

[21] LTE Uplink Level Simulator. [Online]. Available: http://www.nt.tuwien.ac.at/ltesimulator/

[22] M. K. Müller, F. Ademaj, T. Dittrich *et al.*, "Flexible multi-node simulation of cellular mobile communications: The Vienna 5G system level simulator", *EURASIP Journal on Wireless Communications and Networking*, vol. 2018, no.1, pp. 1–17, 2018. DOI: 10.1186/s13638-018-1238-7.

[23] N. M. Balasubramanya, S. Payami, and M. Sellathurai, "Uplink resource allocation for shared LTE and SCMA IoT Systems", in *Proc. of IEEE 87th Vehicular Technology Conference (VTC)*, 2018, pp. 1–5. DOI: 10.1109/vtcspring.2018.8417621.

[24] R. Ruby, V. C. M. Leung, and D. G. Michelson, "Uplink scheduler for SC-FDMA based heterogeneous traffic networks with QoS assurance and guaranteed resource utilization", *IEEE Transactions on Vehicular Technology*, vol. 64, no. 10, pp. 4780–4796, 2015. DOI: 10.1109/TVT.2014.2367007.

[25] N. Trabelsi, L. Roullet, and A. Feki, "A generic framework for dynamic eICIC optimization in LTE heterogeneous networks", in *Proc. of IEEE 80th Vehicular Technology Conference (VTC)*, 2014, pp. 1–6. DOI: 10.1109/VTCFall.2014.6965814.

[26] F. Ren, Y. Xu, H. Yang, J. Zhang, and C. Ling, "Frequency domain packet scheduling stability analysis for 3GPP LTE uplink", *IEEE Transactions on Mobile Computing*, vol. 12, no. 12, pp. 2412–2426, 2013. DOI: 10.1109/TMC.2012.223.

[27] H. Sahlin, "Channel prediction for link adaptation in LTE uplink", in *Proc. of IEEE Vehicular Technology Conference*, 2012, pp. 1–5. DOI: 10.1109/VTCFall.2012.6398940.

[28] J. Blumenstein, J. C. Ikuno, J. Prokopec, and M. Rupp, "Simulating the long term evolution uplink physical layer", in *Proc. of IEEE 53rd International Symposium (ELMAR 2011)*, 2011, pp. 141–144.

[29] Multiplexing and channel coding for Evolved Universal Terrestrial Radio Access (E-UTRA), 3GPP TS 36.212, v14.2.0, 2017.

[30] S. Kasapovic, S. Mujkic, and S. Mujacic, "Enhanced MIMO influence on LTE-Advanced networks performances", *Elektronika ir Elektrotechnika*, vol. 22, no. 1, pp. 81–86, 2016. DOI: 10.5755/J01.EEE.22.1.7698.

[31] M. Q. Abdulhasan, M. I. Salman, C. K. Ng, N. K. Noordin, S. H. Hashim, and F. Hashim, "An adaptive threshold feedback compression scheme based on channel quality indicator (CQI) in long term evolution (LTE)", *SPRINGER Wireless Personal Communications*, vol. 82, no. 4, pp. 2323–2349, 2015. DOI: 10.1007/s11277-015-2350-1.

[32] Physical layer procedures for Evolved Universal Terrestrial Radio Access (E-UTRA), 3GPP TS 36.213, v14.2.0, 2017.

[33] M. Jar and G. Fettweis, "Throughput maximization for LTE uplink via resource allocation", in *Proc. of IEEE International Symposium on Wireless Communication Systems (ISWCS)*, 2012, pp. 146–150. DOI: 10.1109/iswcs.2012.6328347.

[34] M. Algharem, M. H. Omar, I. Aldmour, and R. Budiarto, "Multicast resource allocation with opportunistic scheduling in LTE networks", *Elektronika ir Elektrotechnika*, vol. 24, no. 5, pp. 92–101, 2018. DOI: 10.5755/J01.EIE.24.5.21850.

[35] V. Shivaldova, G. Maier, D. Smely, N. Czink, A. Paier, and C. F. Mecklenbräuer, "Performance analysis of vehicle-to-vehicle tunnel measurements at 5.9 GHz", in *General Assembly and Scientific Symposium of International Union of Radio Science (URSI)*, 2011, pp. 1–4, 2011. DOI: 10.1109/URSIGASS.2011.6050543.

[36] V. Shivaldova, A. Winkelbauer, and C. F. Mecklenbräuker, "Signal-to-noise modelling for vehicle-to-infrastructure communications", in *Proc. of IEEE 6th International Symposium on Wireless Vehicular Communications (WiVeC2014)*, 2014, pp. 1–5. DOI: 10.1109/WIVEC.2014.6953260.

[37] *LTE Measurements*. Available: DOI: 10.17028/rd.lboro.12984542.